
Branching Ratio and CP Asymmetry of $B_s \rightarrow K_0^*(1430)\pi$ Decays in the PQCD Approach

ZHI-QING ZHANG

*Department of Physics, Henan University of Technology,
Zhengzhou, Henan 450052, P.R.China*

PACS 13.25.Hw – Decays of bottom mesons

PACS 12.38.Bx – Perturbative calculations

PACS 14.40.Nd – Bottom mesons

Abstract – In the two-quark model supposition for $K_0^*(1430)$, the branching ratios and the direct CP-violating asymmetries for decays $\bar{B}_s^0 \rightarrow K_0^{*0}(1430)\pi^0$, $K_0^{*+}(1430)\pi^-$ are studied by employing the perturbative QCD factorization approach. We find that although these two decays are both tree-dominated, the ratio of their penguin to tree contributions are very different: there is only a few percent for the decay $\bar{B}_s^0 \rightarrow K_0^{*+}(1430)\pi^-$, while about 37% in scenario I, even 51% in scenario II for the decay $\bar{B}_s^0 \rightarrow K_0^{*0}(1430)\pi^0$. It results that these two decays have very different values in the branching ratios and the direct CP asymmetries. The branching ratio of the decay $\bar{B}_s^0 \rightarrow K_0^{*+}(1430)\pi^-$ is at the order of 10^{-5} , and its direct CP asymmetry is about (20–30)%. While for the decay $\bar{B}_s^0 \rightarrow K_0^{*0}(1430)\pi^0$, its direct CP-violating asymmetry is very large and about 90%, but it is difficult to measure it, because the branching ratio for this channel is small and only 10^{-7} order.

Introduction. – Along with many scalar mesons found in experiments, more and more efforts have been made to study the scalar meson spectrum theoretically [1–7]. There are two typical schemes for their classification [1, 2]. Scenario I (SI): the nonet mesons below 1 GeV, including $f_0(600)$, $f_0(980)$, $K_0^*(800)$, and $a_0(980)$, are usually viewed as the lowest lying $q\bar{q}$ states, while the nonet ones near 1.5 GeV, including $f_0(1370)$, $f_0(1500)/f_0(1700)$, $K_0^*(1430)$, and $a_0(1450)$, are suggested as the first excited states. In scenario II (SII), the nonet mesons near 1.5 GeV are treated as $q\bar{q}$ ground states, while the nonet mesons below 1 GeV are exotic states beyond the quark model, such as four-quark bound states. In order to uncover the inner structures of these scalar mesons, many factorization approaches are used to research the B meson decay modes with a final state scalar meson, such as the generalized factorization approach [8], QCD factorization approach [9–11], and perturbative QCD (PQCD) approach [12–16].

Whether $K_0^{*0}(1430)$ belongs to the first excited state (scenario I) or the lowest lying state (scenario II) is an interesting question, which impacts on its hadronic parameters, such as form factor, decay constant and Gegenbauer moment. For example, the form factor $F_0^{BK_0^*}(q^2)$ is defined as

$$F_0^{BK_0^*}(q^2) = \frac{F_0^{BK_0^*}(0)}{1 - a(q^2/m_B^2) + b(q^2/m_B^2)^2}, \quad (1)$$

where the parameters a, b are obtained from the fitting procedure among the region $0 < q^2 < 10\text{GeV}^2$. They have different values in two scenarios by using the covariant light-front quark model [17], $a = 0.59, b = 0.09$ for scenario I and $a = 0.44, b = 0.05$ for scenario II. From the potential model calculation, we know that the decay constant and the form factor for scenario I have opposite signs [10], while it is not the case for scenario II. From QCD sum rule calculation [18], one can find different masses for the scalar meson $s\bar{q}(q = u, d)$ under the different scenario assumptions: $m(s\bar{q}) = 1.410 \pm 0.049 \text{ GeV}$ for scenario II and $m(s\bar{q}) > 2.0 \text{ GeV}$ for scenario I, so the authors considered that scenario II is more favored. B meson decays offer a promising opportunity to investigate this question: Here $K_0^*(1430)$ can be treated as a $q\bar{q}$ state in both scenarios, it is easy to make quantitative predictions in the two-quark model supposition, so we would like to use the PQCD approach to calculate the branching ratios and the CP-violating asymmetries for decays $\bar{B}_s^0 \rightarrow K_0^{*0}(1430)\pi^0, K_0^{*+}(1430)\pi^-$. Certainly, we use the hadronic parameters derived from QCD sum-rule method in our calculations. Comparing the theoretical prediction with the future experimental data will indicate information on the structure of $K_0^{*0}(1430)$. In the following, $K_0^*(1430)$ is denoted as K_0^* in some places for convenience.

The perturbative QCD calculation. – Under the two-quark model for the scalar meson $K_0^*(1430)$ supposition, the amplitudes for decays $\bar{B}_s^0 \rightarrow K_0^*\pi$ can be conceptually written as the convolution,

$$\begin{aligned} \mathcal{A}(\bar{B}_s \rightarrow K_0^*\pi) \sim & \int dx_1 dx_2 dx_3 b_1 db_1 b_2 db_2 b_3 db_3 \\ & \cdot \text{Tr} \left[C(t) \Phi_{B_s}(x_1, b_1) \Phi_{K_0^*}(x_2, b_2) \Phi_\pi(x_3, b_3) H(x_i, b_i, t) S_t(x_i) e^{-S(t)} \right], \end{aligned} \quad (2)$$

where $b_i(i = 1, 2, 3)$ is the conjugate space coordinate of k_{iT} , and t is the largest energy scale in function $H(x_i, b_i, t)$. Here Tr denotes the trace over Dirac and color indices, $C(t)$ is the Wilson coefficient evaluated at scale t , which includes the hard dynamics being from m_W scale down to $t \sim \mathcal{O}(\sqrt{\Lambda M_{B_s}})$. The function $H(k_1, k_2, k_3, t)$ describes the six-quark hard scattering kernel, which consists of the effective four quark operators and a hard gluon to connect the spectator quark in the decay. In order to smear the end-point singularity on x_i , the jet function $S_t(x)$ [20], which comes from the resummation of the double logarithms $\ln^2 x_i$, is used. The last term $e^{-S(t)}$ is the Sudakov form factor which suppresses the soft dynamics effectively [21]. So this hard part H can be perturbatively calculated. Here $x_i(i = 1, 2, 3)$ is the momenta fraction of the antiquark in each meson. There are the same conventions with Refs. [15, 16] in our calculations.

In the standard model, the related weak effective Hamiltonian H_{eff} mediating the $b \rightarrow d$ type transitions can be written as

$$\mathcal{H}_{eff} = \frac{G_F}{\sqrt{2}} \left[\sum_{p=u,c} V_{pb} V_{pd}^* (C_1(\mu) O_1^p(\mu) + C_2(\mu) O_2^p(\mu)) - V_{tb} V_{td}^* \sum_{i=3}^{10} C_i(\mu) O_i(\mu) \right]. \quad (3)$$

where the local four-quark operator $Q_i(i = 1, \dots, 10)$ and the corresponding Wilson coefficient C_i can be found in Ref. [22]. $V_{p(t)b}, V_{p(t)d}$ are the CKM matrix elements.

From the leading order Feynman diagrams for each considered channel, it is easy to get the analytic formulas for the amplitudes corresponding to $(V-A)(V-A)$, $(V-A)(V+A)$ and $(S-P)(S+P)$ operators, which are similar to those of $B \rightarrow f_0(980)K(\pi), f_0(1500)K(\pi)$ [15, 16]. We just need to replace some corresponding wave functions, Wilson coefficients, and parameters.

Combining the contributions from different diagrams, the total decay amplitudes for these decays can be written as

$$\sqrt{2}\mathcal{M}(K_0^{*0}\pi^0) = \xi_u [M_{eK_0^*} C_2 + F_{eK_0^*} a_2] - \xi_t \left[F_{eK_0^*} \left(-a_4 - \frac{1}{2}(3C_7 + C_8) + \frac{5}{3}C_9 + C_{10} \right) \right]$$

$$\begin{aligned}
 & + F_{eK_0^*}^{P2} (a_6 - \frac{1}{2}a_8) + M_{eK_0^*} \left(-\frac{C_3}{3} + \frac{C_9}{2} + \frac{3C_{10}}{2} \right) - (M_{eK_0^*}^{P1} + M_{aK_0^*}^{P1}) \\
 & \times (C_5 - \frac{C_7}{2}) + M_{eK_0^*}^{P2} \frac{3C_8}{2} - M_{aK_0^*} (C_3 - \frac{1}{2}C_9) - F_{aK_0^*} (a_4 - \frac{1}{2}a_{10}) \\
 & - F_{aK_0^*}^{P2} (a_6 - \frac{1}{2}a_8) \Big] , \tag{4}
 \end{aligned}$$

$$\begin{aligned}
 \overline{\mathcal{M}}(K_0^{*+}\pi^-) = & \xi_u [M_{eK_0^*} C_1 + F_{eK_0^*} a_1] - \xi_t \left[F_{eK_0^*} (a_4 + a_{10}) + F_{eK_0^*}^{P2} (a_6 + a_8) \right. \\
 & + M_{eK_0^*} (C_3 + C_9) + M_{eK_0^*}^{P1} (C_5 + C_7) + M_{aK_0^*} (C_3 - \frac{1}{2}C_9) \\
 & \left. + M_{aK_0^*}^{P1} (C_5 - \frac{1}{2}C_7) + F_{aK_0^*} (a_4 - \frac{1}{2}a_{10}) + F_{aK_0^*}^{P2} (a_6 - \frac{1}{2}a_8) \right] , \tag{5}
 \end{aligned}$$

where $F_{e(a)K_0^*}$ and $M_{e(a)K_0^*}$ are the π meson emission (annihilation) factorizable contributions and nonfactorizable contributions from penguin operators respectively. The upper label T denotes the contributions from the tree operators. $P1$ and $P2$ denote the contributions from the $(V-A)(V+A)$ and $(S-P)(S+P)$ type operators, respectively. The others are the contributions from the $(V-A)(V-A)$ type ones. The combinations of the Wilson coefficients are defined as usual:

$$\begin{aligned}
 a_1(\mu) &= C_2(\mu) + \frac{C_1(\mu)}{3}, \quad a_2(\mu) = C_1(\mu) + \frac{C_2(\mu)}{3}, \\
 a_i(\mu) &= C_i(\mu) + \frac{C_{i+1}(\mu)}{3}, \quad i = 3, 5, 7, 9, \\
 a_i(\mu) &= C_i(\mu) + \frac{C_{i-1}(\mu)}{3}, \quad i = 4, 6, 8, 10. \tag{6}
 \end{aligned}$$

Numerical results and discussions. – In the two-quark picture, the scalar decay constant $\bar{f}_{K_0^*}$ for the scalar meson K_0^* can be defined as

$$\langle K_0^*(p) | \bar{q}_2 q_1 | 0 \rangle = m_{K_0^*} \bar{f}_{K_0^*}, \tag{7}$$

where $m_{K_0^*}(p)$ is the mass (momentum) of K_0^* . The light-cone distribution amplitudes for the scalar meson K_0^* can be written as

$$\begin{aligned}
 \langle K_0^*(p) | \bar{q}_1(z)_l q_2(0)_j | 0 \rangle = & \frac{1}{\sqrt{2N_c}} \int_0^1 dx e^{ixp \cdot z} \\
 & \times \{ \not{p} \Phi_{K_0^*}(x) + m_{K_0^*} \Phi_{K_0^*}^S(x) + m_{K_0^*} (\not{n}_+ \not{n}_- - 1) \Phi_{K_0^*}^T(x) \}_{jl}, \tag{8}
 \end{aligned}$$

where n_+ and n_- are lightlike vectors: $n_+ = (1, 0, 0_T)$, $n_- = (0, 1, 0_T)$. The twist-2 light-cone distribution amplitude $\Phi_{K_0^*}$ can be expanded in the Gegenbauer polynomials:

$$\Phi_{K_0^*}(x, \mu) = \frac{\bar{f}_{K_0^*}(\mu)}{2\sqrt{2N_c}} 6x(1-x) \left[B_0(\mu) + \sum_{m=1}^{\infty} B_m(\mu) C_m^{3/2}(2x-1) \right]. \tag{9}$$

As for the twist-3 distribution amplitudes $\Phi_{K_0^*}^S$ and $\Phi_{K_0^*}^T$, we adopt the asymptotic form:

$$\Phi_{K_0^*}^S = \frac{1}{2\sqrt{2N_c}} \bar{f}_{K_0^*}, \quad \Phi_{K_0^*}^T = \frac{1}{2\sqrt{2N_c}} \bar{f}_{K_0^*} (1-2x). \tag{10}$$

The decay constant $\bar{f}_{K_0^*}$ and the Gegenbauer moments B_1, B_3 of distribution amplitudes for $K_0^*(1430)$ have been calculated in the QCD sum rules [10], which are listed as

$$\text{scenarioI : } B_1 = 0.58 \pm 0.07, B_3 = -1.2 \pm 0.08, \bar{f}_{K_0^*} = -(300 \pm 30) \text{ MeV}, \tag{11}$$

$$\text{scenarioII : } B_1 = -0.57 \pm 0.13, B_3 = -0.42 \pm 0.22, \bar{f}_{K_0^*} = (445 \pm 50) \text{ MeV}, \tag{12}$$

Table 1: Decay amplitudes for decays $\bar{B}_s^0 \rightarrow K_0^{*0}(1430)\pi^0, K_0^{*+}(1430)\pi^-$ ($\times 10^{-2}\text{GeV}^3$).

| | $F_{eK_0^*}^T$ | $F_{eK_0^*}$ | $M_{eK_0^*}^T$ | $M_{eK_0^*}$ | $M_{aK_0^*}$ | $F_{aK_0^*}$ |
|---|----------------|--------------|----------------|-----------------|-----------------|----------------|
| $\bar{B}_s^0 \rightarrow K_0^{*0}(1430)\pi^0$ (SI) | -13.4 | -1.2 | $-6.4 + 4.5i$ | $0.15 - 0.08i$ | $-0.04 + 0.08i$ | $-2.7 - 6.5i$ |
| $\bar{B}_s^0 \rightarrow K_0^{*0}(1430)\pi^0$ (SII) | 16.5 | 1.7 | $0.2 + 3.9i$ | $0.01 - 0.09i$ | $0.20 + 0.11i$ | $0.2 + 8.6i$ |
| $\bar{B}_s^0 \rightarrow K_0^{*+}(1430)\pi^-$ (SI) | 121.3 | 0.1 | $4.0 - 2.7i$ | $-0.14 + 0.09i$ | $0.05 - 0.11i$ | $3.8 + 9.1i$ |
| $\bar{B}_s^0 \rightarrow K_0^{*+}(1430)\pi^-$ (SII) | -220.7 | 0.6 | $0.1 - 2.7i$ | $-0.01 + 0.11i$ | $-0.27 - 0.16i$ | $-0.3 - 12.2i$ |

The other input parameters used in the numerical calculations are specified below [23]

$$f_{B_s} = 230\text{MeV}, M_{B_s} = 5.37\text{GeV}, M_W = 80.41\text{GeV}, \quad (13)$$

$$\alpha = 100^\circ \pm 20^\circ, \tau_{B_s} = 1.470 \times 10^{-12}\text{s}, \quad (14)$$

$$|V_{ub}| = 3.93 \times 10^{-3}, V_{ud} = 0.974, \quad (15)$$

$$|V_{td}| = 8.1 \times 10^{-3}, V_{tb} = 1.0. \quad (16)$$

It is noticed that there is dramatic difference for the central value of CKM angle α between the previous and the present PDG values. The present PDG value of α is $89.0^{+4.4}_{-4.2}$ [24], which is shown in the following figures.

In the B_s -rest frame, the decay width of $\bar{B}_s^0 \rightarrow K_0^*(1430)\pi$ can be written as

$$\Gamma = \frac{G_F^2(1 - r_{K_0^*}^2)}{32\pi m_{B_s}} |\bar{\mathcal{M}}|^2, \quad (17)$$

where $\bar{\mathcal{M}}$ is the total decay amplitude of each considered decay, which has been given in the previous section, and the mass ratio $r_{K_0^*} = m_{K_0^*}/M_{B_s}$. $\bar{\mathcal{M}}$ can be rewritten as

$$\bar{\mathcal{M}} = V_{ub}V_{ud}^*T - V_{tb}V_{td}^*P = V_{ub}V_{ud}^* \left[1 + ze^{i(-\alpha+\delta)} \right], \quad (18)$$

where α is the Cabibbo-Kobayashi-Maskawa weak phase angle, and δ is the relative strong phase between the tree and the penguin amplitudes, which are denoted as "T" and "P," respectively. The term z describes the ratio of penguin to tree contributions and is defined as

$$z = \left| \frac{V_{tb}V_{td}^*}{V_{ub}V_{ud}^*} \right| \left| \frac{P}{T} \right|. \quad (19)$$

If one relates $\bar{\mathcal{M}}$ with \mathcal{M} , which is the total decay amplitude for the corresponding conjugated decay mode, it is easy to rewrite the decay width Γ as

$$\Gamma = \frac{G_F^2(1 - r_{K_0^*}^2)}{32\pi m_{B_s}} |V_{ub}V_{ud}^*T|^2 [1 + 2z \cos \alpha \cos \delta + z^2]. \quad (20)$$

So the CP-averaged branching ratio for each considered decay is defined as

$$\mathcal{B} = \Gamma \tau_{B_s} / \hbar, \quad (21)$$

where τ_{B_s} is the life time of B_s meson.

Using the input parameters and the wave functions as specified in this section, it is easy to get the values of the factorizable and nonfactorizable amplitudes from the emission and annihilation topology diagrams of the considered decays in both scenarios, which are listed in Table 1. It is noticed that each penguin amplitude in the table includes the contributions from three kinds of operators. The emission factorizable and nonfactorizable diagram

Table 2: CP-averaged branching ratios and direct CP asymmetries of decays $\bar{B}_s^0 \rightarrow K_0^{*0}(1430)\pi^0, K_0^{*+}(1430)\pi^-$. The theoretical errors of branching ratios correspond to the uncertainties due to variation of (i) the B_s meson shape parameter ω_b , (ii) the decay constant $\bar{f}_{K_0^*}$, (iii) the Gegenbauer moments B_1 and B_3 of the scalar meson K_0^* . While the errors of direct CP asymmetries are mainly from (i), (iii) and the CKM angle $\alpha = (100 \pm 20)^\circ$.

| | Branching ratios | Direct CP asymmetries (in %) |
|---|--|---------------------------------------|
| $\bar{B}_s^0 \rightarrow K_0^{*0}(1430)\pi^0$ (SI) | $(4.5^{+1.4+0.9+0.4}_{-1.1-0.9-0.4}) \times 10^{-7}$ | $93.6^{+4.8+1.0+0.0}_{-7.3-1.0-8.7}$ |
| $\bar{B}_s^0 \rightarrow K_0^{*0}(1430)\pi^0$ (SII) | $(4.1^{+1.0+1.0+0.6}_{-0.7-0.1-0.6}) \times 10^{-7}$ | $95.5^{+1.2+3.4+4.0}_{-8.7-4.1-13.9}$ |
| $\bar{B}_s^0 \rightarrow K_0^{*+}(1430)\pi^-$ (SI) | $(1.2^{+0.5+0.2+0.1}_{-0.3-0.2-0.1}) \times 10^{-5}$ | $28.1^{+4.9+0.7+0.0}_{-4.4-0.7-2.4}$ |
| $\bar{B}_s^0 \rightarrow K_0^{*+}(1430)\pi^-$ (SII) | $(3.7^{+1.4+0.9+0.8}_{-1.0-0.8-0.7}) \times 10^{-5}$ | $21.0^{+3.4+2.1+0.0}_{-3.1-2.5-2.5}$ |

contributions from the tree operators are dominant. In the decay $\bar{B}_s^0 \rightarrow K_0^{*+}(1430)\pi^-$, the amplitude $F_{eK_0^*}^T$ is enhanced by the large Wilson coefficients $C_2 + C_1/3$, which induce the tree operator contributions to be absolutely dominant and the ratio P/T is only 8% in scenario I, 5.5% in scenario II. Certainly, for the other channel $\bar{B}_s^0 \rightarrow K_0^{*0}(1430)\pi^0$, the Wilson coefficients associated with the amplitude $F_{eK_0^*}^T$ are $C_2/3 + C_1$, which are color suppressed. We know that the sign of $C_2/3$ is positive while the sign of C_1 is negative, which can cancel each other mostly. So the amplitude $F_{eK_0^*}^T$ is highly suppressed compared with the one for the channel $\bar{B}_s^0 \rightarrow K_0^{*+}(1430)\pi^-$. So that the influence from the penguin contributions becomes important in the decay $\bar{B}_s^0 \rightarrow K_0^{*0}(1430)\pi^0$. The penguin operator contributions are mainly from the factorizable emission diagrams and annihilation diagrams, the latter are more important and provide a large imagine part, which often induces a large direct CP-violating asymmetry (shown in Table 2). From Table 1, one can find that the ratio P/T for the decay $\bar{B}_s^0 \rightarrow K_0^{*0}(1430)\pi^0$ is large and about 37% for scenario I, 51% for scenario II.

Using the amplitudes as specified in Table 1, we can calculate the branching ratios of the considered modes, which are listed in Table 2. The uncertainties are mainly from the B_s meson shape parameter ω_b , the decay constant $\bar{f}_{K_0^*}$, the Gegenbauer moments B_1 and B_3 of the scalar meson K_0^* . From the results, one can find that the branching ratio of the decay channel $\bar{B}_s^0 \rightarrow K_0^{*+}(1430)\pi^-$ is about two order lager than that of $\bar{B}_s^0 \rightarrow K_0^{*0}(1430)\pi^0$. It is because that the former receives a much larger π^0 emission factorizable diagram amplitude

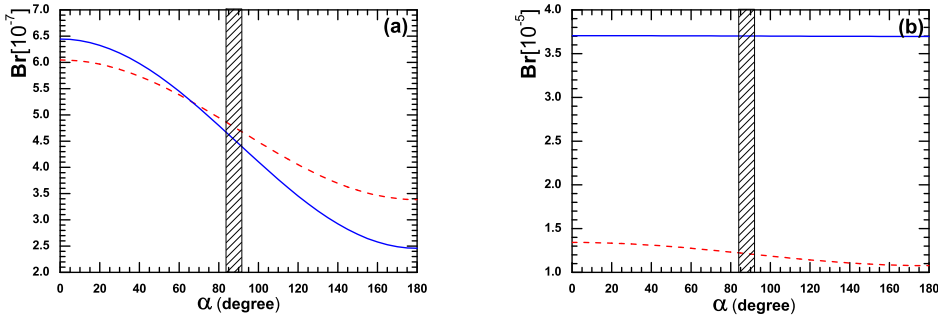


Fig. 1: The dependence of the branching ratios for $\bar{B}_s^0 \rightarrow K_0^{*0}(1430)\pi^0$ (a) and $\bar{B}_s^0 \rightarrow K_0^{*+}(1430)\pi^-$ (b) on the Cabibbo-Kobayashi-Maskawa angle α . The dashed (solid) curves are plotted in scenario I (II). The vertical bands show the range of $\alpha: 89.0^{+4.4}_{-4.2}$ [24].

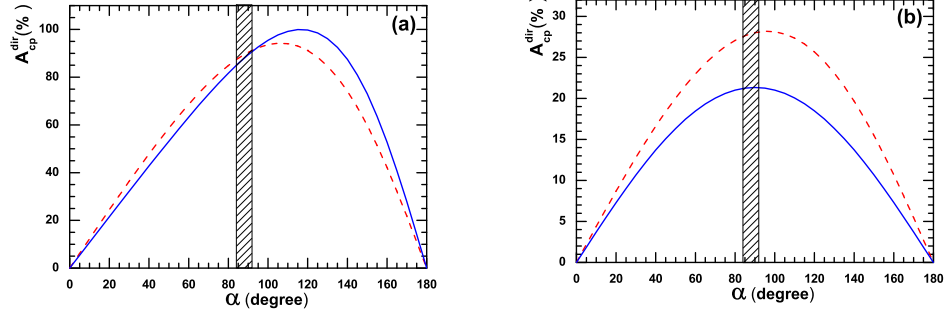


Fig. 2: The dependence of the direct CP-violating asymmetries for $\bar{B}_s^0 \rightarrow K_0^{*0}(1430)\pi^0$ (a) and $\bar{B}_s^0 \rightarrow K_0^{*+}(1430)\pi^-$ (b) on the Cabibbo-Kobayashi-Maskawa angle α . The dashed (solid) curves are plotted in scenario I (II). The vertical bands show the range of α : $89.0^{+4.4}_{-4.2}$ [24].

than the latter. It is interesting to contrast the predictions for decays $\bar{B}_s^0 \rightarrow K_0\pi$ and those for $\bar{B}_s^0 \rightarrow K_0^*(1430)\pi$, it seems to exist some similar point: the QCD factorization approach predicted the branching ratio of the decay $\bar{B}_s \rightarrow K_0^+\pi^-$ was about $(1.02^{+0.59}_{-0.52}) \times 10^{-5}$ and $(4.9^{+6.3}_{-3.5}) \times 10^{-7}$ [25] for the decay $\bar{B}_s^0 \rightarrow K_0^0\pi^0$. Certainly, the present experimental result for the decay $\bar{B}_s \rightarrow K_0^+\pi^-$ is about $(5.0 \pm 1.1) \times 10^{-6}$ [19]. If the future experimental value for the decay $\bar{B}_s^0 \rightarrow K_0^{*+}(1430)\pi^-$ also falls into 10^{-6} order, which is less than our prediction, it is might because the following two reasons: First, the value of the transition from factor $\bar{B}_s^0 \rightarrow K_0^*(1430)$ predicted by the PQCD approach is larger than the data. Second, we only calculate in the leading-order. The higher order contributions might give some corrections to the leading order results. Some contributions from the next-to-leading-order (NLO) corrections have been calculated for the decays $B \rightarrow K\pi$ [26], and the results show that their branching ratios decrease by about 20% after including the NLO effects. These effects might also have an influence on our considered decays.

The dependence of the branching ratios for the decays $\bar{B}_s^0 \rightarrow K_0^{*0}(1430)\pi^0$ and $\bar{B}_s^0 \rightarrow K_0^{*+}(1430)\pi^-$ on the Cabibbo-Kobayashi-Maskawa angle α is displayed in Fig.1. Compared with Fig.1(a), we know that the branching ratio of the decay $\bar{B}_s^0 \rightarrow K_0^{*+}(1430)\pi^-$ is insensitive to the angle α , which is shown in Fig.1(b). From the definition of the CP-averaged branching ratio shown in Eq.(21), one can find that if the branching ratio is insensitive to the angle α , the coefficient of $\cos \alpha$ must be near zero. For the decay $\bar{B}_s^0 \rightarrow K_0^{*+}(1430)\pi^-$, the value of z is very small in both scenarios, about $0.1 \sim 0.2$, so z^2 is smaller and can be neglected compared with 1, at the same time, the strong phase angle δ is about 89° in scenario II, so the value of $(1 + 2z \cos \alpha \cos \delta + z^2)$ is close to 1. Although the strong phase angle δ for scenario I is not so large (about 68.6°), the small value of z makes the branching ratio in this scenario also insensitive to α .

Now, we turn to the evaluations of the direct CP-violating asymmetries of the considered decays in the PQCD approach. The direct CP-violating asymmetry can be defined as

$$\mathcal{A}_{CP}^{dir} = \frac{|\overline{\mathcal{M}}|^2 - |\mathcal{M}|^2}{|\mathcal{M}|^2 + |\overline{\mathcal{M}}|^2} = \frac{2z \sin \alpha \sin \delta}{1 + 2z \cos \alpha \cos \delta + z^2}. \quad (22)$$

Using the calculated ratio z and strong phase δ , it is easy to calculate the numerical values of \mathcal{A}_{CP}^{dir} (in unit of 10^{-2}) in two scenarios, which are the listed in Table 2. The uncertainties are mainly from the B_s meson shape parameter $\omega_b = 0.5 \pm 0.05$, the Gegenbauer moments

B_1 and B_3 of the scalar meson K_0^* , the CKM angle $\alpha = (100 \pm 20)^\circ$. For the decay mode $K_0^{*+}(1430)\pi^-$, as discussed above, the value of $(1 + 2z \cos \alpha \cos \delta + z^2)$ is close to 1 in both scenarios, so the corresponding direct CP-violating asymmetry is almost proportional to $\sin \alpha$, that is to say it attains the maximum near 90° (shown in Fig.2b). For the decay mode $K_0^{*0}(1430)\pi^0$, it receives a very large direct CP-violating asymmetry in both scenarios. It is not strange: one can recall that the channel $\bar{B}_s^0 \rightarrow K^0\pi^0$ also receives a large direct CP-violating asymmetry, $(59.4^{+7.9}_{-12.5})\%$ in the pQCD approach [27], about $(41.6^{+47.1}_{-55.8})\%$ predicted by QCDF approach [25].

Conclusion. – In this paper, we calculate the branching ratios and the CP-violating asymmetries of decays $\bar{B}_s^0 \rightarrow K_0^*(1430)\pi$ in the PQCD factorization approach. Using the decay constants and light-cone distribution amplitudes derived from QCD sum-rule method, we find that although these two decays are both tree-dominated, the ratio of their penguin to tree contributions are very different, there is only a few percent for the decay $\bar{B}_s^0 \rightarrow K_0^{*+}(1430)\pi^-$, while about 37% in scenario I, even 51% in scenario II for the decay $\bar{B}_s^0 \rightarrow K_0^{*0}(1430)\pi^0$, which results these two decays have very different values in the branching ratios and the direct CP asymmetries: The branching ratio of the decay $\bar{B}_s^0 \rightarrow K_0^{*+}(1430)\pi^-$ is at the order of 10^{-5} , its direct CP asymmetry is about $(20 - 30)\%$. While for the decay $\bar{B}_s^0 \rightarrow K_0^{*0}(1430)\pi^0$, its direct CP-violating asymmetry is very large and about 90%, but it is difficult to measure it, because the branching ratio for this channel is small and only 10^{-7} order. Between these two scenarios, there is less different for the results of the channel $\bar{B}_s^0 \rightarrow K_0^{*0}(1430)\pi^0$, while larger different for those of $\bar{B}_s^0 \rightarrow K_0^{*+}(1430)\pi^-$, especially from the branching ratio. Because its branching ratio is proportional to the modular square of the tree amplitude, which for scenario II is about 3.1 times that of scenario I. So the decay $\bar{B}_s^0 \rightarrow K_0^{*+}(1430)\pi^-$ can be used to determine the inner structure of $K_0^*(1430)$ by comparing the theoretical prediction with the future experimental data.

This work is partly supported by the National Natural Science Foundation of China under Grant No. 11047158, and by Foundation of Henan University of Technology under Grant No. 2009BS038. The author would like to thank Cai-Dian Lü for helpful discussions.

REFERENCES

- [1] N.A. Tornqvist, Phys. Rev. Lett. **49**, 624 (1982).
- [2] G.L. Jaffe, Phys. Rev. D **15**, 267 (1977); Erratum-ibid. Phys. Rev. D **15** 281 (1977); A.L. Kataev, Phys. Atom. Nucl. **68**, 567 (2005), Yad. Fiz. **68**, 597 (2005); A. Vijande, A. Valcarce, F. Fernandez and B. Silvestre-Brac, Phys. Rev. D **72**, 034025 (2005).
- [3] J. Weinstein , N. Isgur , Phys. Rev. Lett. **48**, 659 (1982); Phys. Rev. D **27**, 588 (1983); **41**, 2236 (1990); M.P. Locher, *et al.*, Eur. Phys. J. C **4**, 317 (1998).
- [4] V. Baru, *et al.*, Phys. Lett. B **586**, 53 (2004).
- [5] L. Celenza, *et al.*, Phys. Rev. C **61** (2000) 035201.
- [6] M. Strohmeier-Presicek, *et al.*, Phys. Rev. D **60** 054010 (1999).
- [7] F.E. Close, A. Kirk, Phys. Lett. B **483** 345 (2000).
- [8] A.K. Giri , B. Mawlong, R. Mohanta Phys. Rev. D **74**, 114001 (2006).
- [9] H.Y. Cheng, K.C. Yang Phys. Rev. D **71**, 054020 (2005).
- [10] H.Y. Cheng , C.K. Chua , K.C. Yang Phys. Rev. D **73**, 014017 (2006).
- [11] H.Y. Cheng, C.K. Chua and K.C. Yang, Phys. Rev. D **77**, 014034 (2008).
- [12] Z.Q. Zhang and Z.J. Xiao, Chin. Phys. C **34**(05), 528 (2010).
- [13] Z.Q. Zhang, J.D. Zhang, Eur. Phys. J. C **67**, 163 (2010).
- [14] Z.Q. Zhang, Phys. Rev. D **82**, 034036 (2010).
- [15] Z.Q. Zhang, Eur. Phys. J. C **69**, 433 (2010).
- [16] Z.Q. Zhang, J. Phys. G **37**, 085012 (2010).
- [17] H.Y. Cheng, C.K. Chua, C.W. Hwang, Phys. Rev. D **69**, 074025 (2004).

- [18] D.S. Du, J.W. Li, M.Z. Yang, Phys. Lett. B **619**, 105 (2005).
- [19] Heavy Flavor Averaging Group, <http://www.slac.stanford.edu/xorg/hfag>.
- [20] H.n. Li, Phys. Rev. D **66**, 094010 (2002).
- [21] H.n. Li and B. Tseng, Phys. Rev. D **57**, 443 (1998).
- [22] G. Buchalla , A. J. Buras , M. E. Lautenbacher, Rev. Mod. Phys. **68**, 1125 (1996).
- [23] Particle Data Group, C. Amsler, *et al.*, Phys. Lett. B **667**, 1 (2008).
- [24] Particle Data Group, K. Nakamura *et al.*, J.Phys.G **37**, 075021 (2010).
- [25] M. Beneke, M. Neubert, Nucl. Phys.B **675**, 333 (2001).
- [26] H.n. Li, S. Mishima and A.I. Sanda, Phys.Rev.D **72**, 114005 (2005).
- [27] A. Ali, *et al.*, Phys. Rev. D **76**, 074018 (2007).